PARAMETRIC ANALYSIS OF A PHENOMENOLOGICAL MODEL FOR VORTEX-INDUCED MOTIONS OF MONOCOLUMN PLATFORMS

Guilherme F. Rosetti (guilherme.feitosa@tpn.usp.br)
Rodolfo T. Gonçalves (rodolfo_tg@tpn.usp.br)
André L. C. Fujarra (afujarra@usp.br)
Kazuo Nishimoto (knishimo@usp.br)
Department of Naval Architecture and Ocean Engineering,
Escola Politécnica – University of São Paulo,
Av. Prof. Mello Moraes, 2231, Cidade Universitária,
São Paulo, SP, 05508-900, Brazil

Marcos D. Ferreira (marcos.donato@petrobras.com.br)
Research and Development Center (CENPES)
PETROBRAS
Rio de Janeiro, RJ, Brazil

Abstract. *Phenomenological models are an important branch in VIV and VIM studies, as CFD is not yet a suitable tool for intense use in engineering analysis. In the present paper, a phenomenological model for evaluating the VIM of monocolumn platforms is presented and its results are compared with experimental results. The main objective of the paper is to present a parametric analysis, having in mind the physical significance of the proposed modifications. The parameters varied are: Aspect ratio (L/D), structural damping, fluid damping and Strouhal number (S).*
The results are presented in terms of: non-dimensional amplitudes of motion (A_X/D and A_Y/D), added mass coefficient (C_a) and periods of motion (T_X and T_Y).
The model is based on a time-domain, two degree-of-freedom structural model coupled with a van der Pol type wake oscillator. The governing equations are solved through RK4 schemes.

Keywords*: Vortex-induced motion, phenomenological model, van der Pol wake oscillator, two degree-of-freedom, monocolumn platform*

NOMENCLATURE

ε_x	Damping coefficient for inline oscillator
ε_y	Damping coefficient for cross-flow oscillator
ξ	Structural damping coefficient
ρ	Fluid density [kg/m3]
ω	Frequency of oscillation [rad/s]
γ	Damping coefficient
Ω_f	Strouhal frequency [rad/s]
Ω_s	Natural frequency [rad/s]
A_x	Coupling amplification drag parameter
A_y	Coupling amplification lift parameter
A_X/D	Reduced inline displacement
A_Y/D	Reduced cross-flow displacement
C_0	Drag coefficient for fixed cylinder
C_a	Added mass coefficient
$C_{D,amp}$	Amplified drag
C_D	Drag coefficient
C_L	Lift coefficient
C_{L0}	Vortex shedding lift coefficient
C_M	Potential added mass coefficient
C_{i0}	Vortex shedding drag coefficient
c_f	Fluid damping [kg/s]
c_s	Structural damping [kg/s]
D	Diameter[m]
K	Coupling parameter
k	Stiffness [N/m]
L	Immersed length [m]
m_f	Potential added mass [kg]
m_s	Structural mass [kg]

q_x	Reduced drag coefficient
q_y	Reduced lift coefficient
S	Strouhal number
T_0	Natural period of oscillation in calm waters
T_X	Period of inline motion [s]
T_Y	Period of cross-flow motion [s]
V, U	Flow velocity [m/s]
V_r, V_{r0}	Reduced velocity in calms waters
x	Inline displacement [m]
y	Cross-flow displacement [m]

1. INTRODUCTION

This paper presents a numerical tool based on a phenomenological model adapted to represent the fluid-structure interaction of monocolumn platforms during the occurrence of Vortex-Induced Motions. A parametric analysis is performed comparing the results with data from the VIM tests carried out with the MonoBR platform.

The model is composed by a linear two degree-of-freedom oscillator representing the structure dynamic and a non-linear oscillator representing the effect of the vortex shedding and based on the van der Pol´s equation.

The approach considered is to study systematically the effects of varying the parameters which are important to the phenomenon in such a way to get some insight of it.

The work herein presented is being developed in the context of a large effort to study the VIM phenomenon both numerically and experimentally. It is in a very early stage of development as the model is yet quite simple, however, based on a structured line of work where each improvement is implemented carefully and compared with experimental results. During this process, hopefully both approaches, numerical and experimental, can interact and improve themselves. With these aspects in mind, the present paper was structured in such a way that useful conclusions can easily be drawn.

The section 2 presents, briefly, the derivation of the model with the theoretical aspects. In section 3 the geometry and parameter values for the model are presented. The results of a parametric analysis are presented in the section 4, with comparisons and discussion. And finally, the last section presents an overview of the results with a brief conclusion.

2. DERIVATION OF THE MODEL

In the present model, a two degree-of-freedom elastically supported rigid cylinder with low aspect ratio was considered, according to details found in Rosetti, G.F. *et al.* (2009). It is allowed to oscillate in both directions, the stream (x-axis) and the cross-wise (y-axis).The free-stream velocity is V, diameter is D and the immersed length is L.

Considering this system, the equation for modeling the structural dynamics can be represented by a linear oscillator as follows:

$$m\ddot{r} + c\dot{r} + kr = F \tag{1}$$

As usual, the inertia and damping forces are both composed by structural and fluid terms, and the stiffness of the system represented by a linear term proportional to the constant k:

$$m = m_s + m_f \tag{2}$$

The fluid component of the inertia corresponds to the potential effects, where the potential added mass reads:

$$m_f = C_M \rho D^2 \pi L/4, \quad C_M = 1 \tag{3}$$

The damping component is linear and also composed by a structural term (viscous dissipation of the support system) and by a fluid damping term:

$$c = c_s + c_f \tag{4}$$

The structural damping term reads

$$c_s = 2m\Omega_s\xi \tag{5}$$

The term Ω_s is the angular natural frequency $\Omega_s = \sqrt{k/m}$ and ξ is the structural damping coefficient.

During the oscillations, the fluid damping term models viscous damping of the structure, which is not provided by vortex shedding. Following Blevins, R.D. (1990), the fluid damping term reads:

$$c_f = \gamma\Omega_f\rho LD^2, \tag{6}$$

where γ is a function of the amplitude , related to the average drag coefficient obtained from cross-flow oscillations. This parameter is here assumed constant, as done by Facchinetti, M.L. *et al.* (2004) among others.

The parameter Ω_f is a reference angular frequency, named Strouhal frequency and, in this case, assumed:

$$\Omega_f = 2\pi S\frac{V}{D}, \tag{7}$$

where S is the Strouhal number.

The effects caused by vortex shedding are modeled by the term on the right-hand side of the dynamic equation. This term reads:

$$F = \frac{1}{2}\rho V^2 DLC_T \tag{8}$$

The displacement variable r is a complex number in which $r = x + iy$, whereas $C_T = C_D + iC_L$.

As mentioned, the oscillatory nature of the motions caused by the interaction between vortex shedding and structure is modeled through van der Pol´s equations. Both cross-flow and inline directions have their own oscillators and the coupling between the two DOF will be presented as follows. The fluid oscillator equations read:

$$\ddot{q}_y + \varepsilon_y\Omega_f^2\left(q_y^2 - 1\right)\dot{q}_y + \Omega_f^2 q_y = \frac{A_y}{D}\ddot{y} \tag{9}$$

$$\ddot{q}_x + \varepsilon_x\Omega_f^2(q_x^2 - 1)\dot{q}_x + 4\Omega_f^2 q_x = \frac{A_x}{D}\ddot{x} \tag{10}$$

The terms on the right-hand side of equations (9) and (10) are the coupling between the fluid oscillator and the structure oscillator. Such terms are functions of the body acceleration, as recommended by Facchinetti, M.L. *et al.* (2004). The counterpart of the coupling between the oscillators is through the lift and drag coefficients

$$C_L = C_{L0}q_y/2 \tag{11}$$

$$C_D = C_0(1 + Kq_x^2) + C_{i0}q_y/2 \tag{12}$$

The constants C_{L0} and C_{i0} are vortex shedding lift and drag coefficients for a fixed structure, C_0 is the drag coefficient for a cylinder at rest and K is a constant determined by fitting the data with the experiments.

3. BASIC GEOMETRY AND PARAMETER VALUES

The experimental test was carried out with a circular structure with low aspect ratio. The dimensions of the small-scale model employed in the numeric model are $L = 0.21\text{m}, D = 0.54\text{m}$.. The immersed length L refers to the full draft configuration. The aspect ratio of this system is, therefore, around 0.4, which is the feature that makes this structure somewhat peculiar, as far as VIM-subjected systems are concerned. The details of the MonoBR tests, such as geometry of the hull and test conditions, were presented in Fujarra, A.L.C. *et al.* (2009).

In the structure oscillator, the structural mass in air is 45.71kg; the structural damping coefficient is a given parameter estimated as 4.4% and the stiffness constant is 4.05N/m. Concerning this last value it's important to emphasize that it refers to the stiffness obtained from decay test in still waters, which means that this is not the stiffness observed with a flow velocity different from zero. It is obvious that each velocity presents a respective stiffness that determines the equilibrium point around which oscillations occur.

The model tests occurred in the Reynolds range $10^4 < Re < 10^5$ and, as usual, the reference vortex shedding lift coefficient C_{L0} is taken as $C_{L0} = 0.3$ as in Blevins, R.D. (1990), Facchinetti, M.L. *et al.* (2004) and Furnes, G. (2000).

The work by Fox, T.A. and West, G.S. (1993) presented results of drag coefficients for a stationary cylinder in a range of Reynolds similar to the present work, testing many aspect ratios. They showed that, below aspect ratio 13, drag coefficient varies dramatically. Corroborating this data, the results obtained from the model tests in Gonçalves, R.T. *et al.* (2009a) were also different from the usual value ($C_0 = 1.2$). According to this, the reference drag C_0 is taken as $C_0 = 0.7$, which was obtained from the experiments reported in Fujarra, A.L.C. *et al.* (2009).

The same work by Fox, T.A. and West, G.S. (1993) showed that, despite a range of Reynolds being usually associated with a Strouhal number equal to 0.2, for low aspect ratios (below 13), this number falls dramatically. The experiments executed in 2008 and reported in Fujarra, A.L.C. *et al.* (2009) corroborated this result by presenting $S = 0.078$. The Strouhal number was identified as being one very important parameter for the present study and will be discussed later.

Following Furnes, G. and Sorensen, K. (2007), the parameter C_{i0} was chosen as $C_{i0} = 0.1$. This value is probably also a function of the aspect ratio; however, there is no public data available for the aspect ratio of the present system.

In order to be completely coherent when using such parameters, all the values should not only be for the same Reynolds range but also for the same aspect ratio. However, there is no available data with all parameters required by the model.

As presented before, the parameter γ was derived by Blevins, R.D. (1990) as

$$\gamma = \frac{C_{D,amp}}{4\pi S} \tag{13}$$

In the present model, the values are not defined per unit length. Therefore, the parameter γ would be $\gamma = 2.14$. In order to be consistent with other authors, for example: Blevins, R.D. (1990) and Facchinetti, M.L. *et al.* (2004), the parameter γ is re-defined as:

$$\gamma = \frac{C_{D,amp}}{4\pi S} L \tag{14}$$

The result $\gamma = 0.45$ is used in the model.

The parameters $A_y, A_x, \varepsilon_y, \varepsilon_x, K_i$ are obtained by fitting the experiments. Therefore, $A_y = 6$; $A_x = 12, \varepsilon_y = 0.15, \varepsilon_x = 0.3, K = 0.05$. Notice that the ratios A/ε are kept equal to 40, as Facchinetti, M.L. *et al.* (2004) obtained from least-square approximation with experimental data.

All these parameters refer to the basic set according to all the following results were obtained.

3. RESULTS AND DISCUSSION

3.1. Definition of analysed cases

As this study is a branch of a combined experimental-numerical study some aspects were considered to be insightful. This approach aims to build a more extensive body of knowledge about the VIM of monocolumn platforms or, more generally, the VIV of cylinders with low aspect ratio. More details about the relevant aspects in VIM phenomenon was explained in Gonçalves, R.T. *et al.* (2009b). Furthermore, by investigating the effects of varying such parameters, one tries to identify the right questions and, through suitable experiments, might be able to answer them.

The following parameters were investigated:

Table 1: Summary of analysed cases

Cases	*Aspect ratio (L/D)*	*Structural damping (ξ)*	*Fluid damping (γ)*	*Strouhal Number (S)*	*Mass Ratio(m*)*	*Natural Period(s)*
Aspect ratio (L/D)	*0.1/0.2/0.3/0.4/0.5/ 0.75/1.0/1.5*	*4.4%*	*0.45*	*0.078*	*1.0*	*~30*
Structural damping (ξ)	*0.4*	*0.44%/2.2%/4.4%/ 8.8%/44%*	*0.45*	*0.078*	*1.0*	*~30*
Fluid damping (γ)	*0.4*	*4.4%*	*0.225/0.45/0.9*	*0.078*	*1.0*	*~30*
Strouhal Number (S)	*0.4*	*4.4%*	*0.45*	*0.05/0.075/0.1/0.15/0. 2/0.25*	*1.0*	*~30*

3.2. Variation of aspect ratio

The first parameter varied in this study was the aspect ratio. The premises of this study were to keep the mass ratio close to unity and keep the same natural period in all the runs.

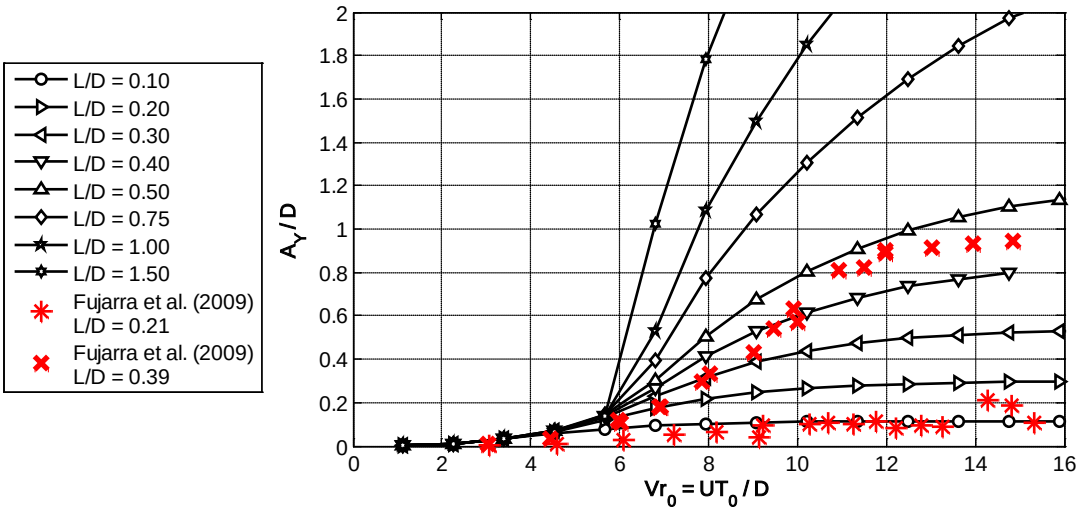

Figure 1: Cross-flow response for different aspect ratios (L/D). Red points are results from model tests

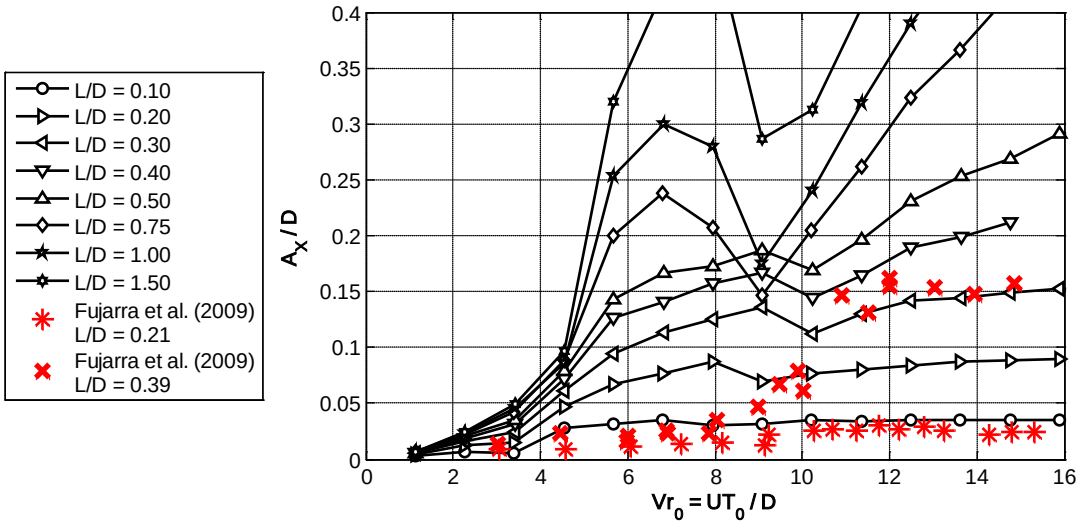

Figure 2: Inline response for different aspect ratios (L/D). Red points are results from model tests

The following results are reduced amplitudes of motions inline and cross-flow, respectively presented in Figure 1 and in Figure 2.

The results show an increase of the amplitudes with the increase of the aspect ratio. The experimental results suggest that this behavior is coherent, as for increasing aspect ratio, there is also an increase of amplitude in both directions. There is, however, a difference in inline direction, where the motions increase earlier than in the experimental results. This requires further investigation, but might be related to the modeling of the inline degree-of-motion or to the Strouhal number in this range.

The next plot, Figure 3, presents the results of added mass for different aspect ratios. The added mass is obtained by a frequency domain analysis procedure as in Fujarra, A.L.C. and Pesce, C.P. (2002) as follows:

$$\frac{\mathcal{F}\left[F_{Hy}\right]}{\mathcal{F}\left[\ddot{Y}\right]} \approx -m_a(\omega) + \frac{ic_v(\omega)}{\omega} \tag{15}$$

where F_{Hy} is the total hydrodynamic force, including potential added mass and fluid damping. Therefore, it arrives:

$$C_a^{FD} = C_a^{FD}(\omega) = \frac{-\Re\left\{\dfrac{\mathcal{F}\left[F_{Hy}\right]}{\mathcal{F}\left[\ddot{Y}\right]}\right\}}{m} \tag{16}$$

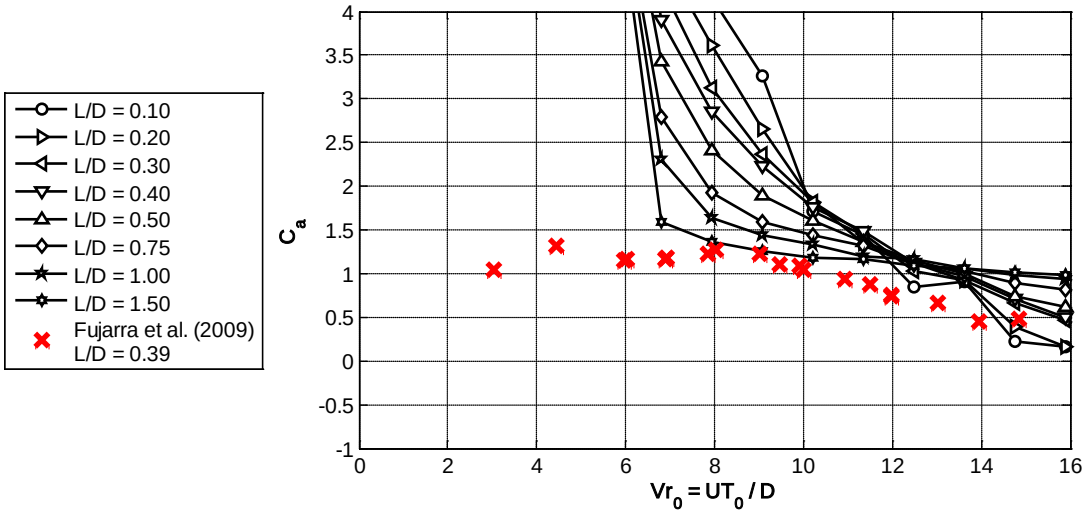

Figure 3: Added mass for different aspect ratios (L/D). Red points are results from model tests

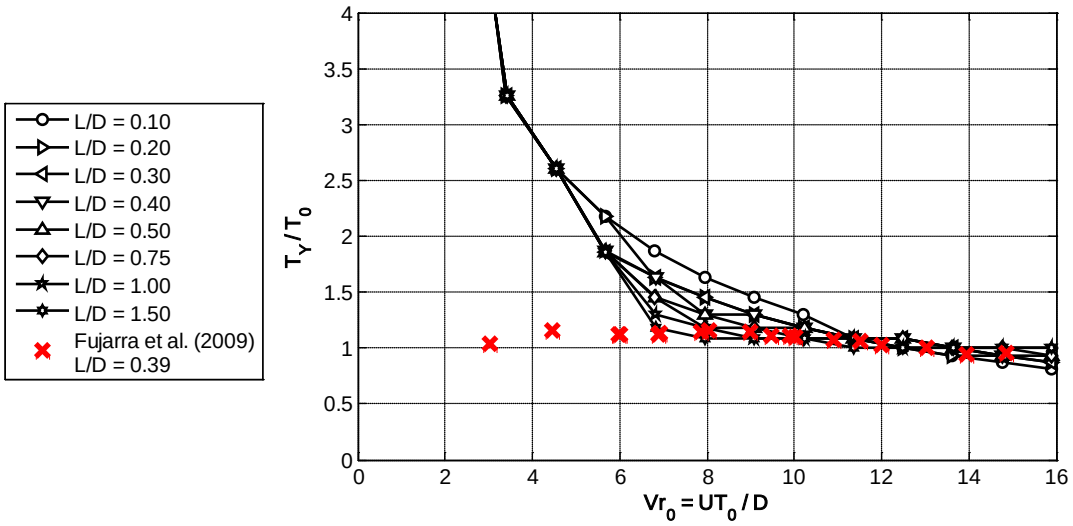

Figure 4: Cross-flow period of oscillation over natural period for different aspect ratios (L/D). Red points are results from model tests

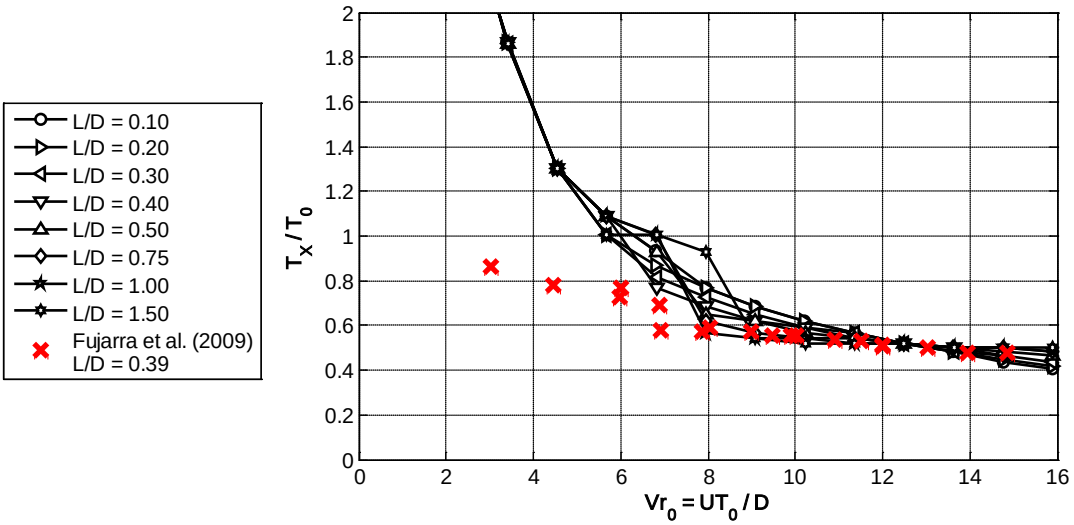

Figure 5: Inline period of oscillation over natural period for different aspect ratios (L/D). Red points are results from model tests

Mainly in high reduced velocities, larger than 8.0, the model reproduces fairly well the behavior of the added mass as obtained by Fujarra, A.L.C. and Pesce, C.P. (2002) and by Vikestad, K., Vandiver, J.K. and Larsen, C.M. (2000). For reduced velocities smaller than that, it is difficult to obtain the added mass from the experimental data, as the amplitudes and forces are very small. This might explain the discrepancy between the model and the experimental results in that region of velocities.

It is very interesting to notice that added mass tend to zero instead of -1. In this sense, the present results differ somewhat from common VIV results and the experimental results presented seem to corroborate this tendency. At this point, it is difficult to understand this difference but further investigation is also being performed.

The next results, Figure 4 and Figure 5, present the period of oscillations cross-flow and inline, respectively.

There is a good correspondence between experimental and numerical results for reduced velocities larger than 8.0 and double-frequency (or half period) relation between inline and cross-flow motions is preserved.

For reduced velocities smaller than 8.0, the model exhibits large periods, due to the modeling of force caused by vortex shedding. In this range ($0.0 < V_{r0} < 8.0$), the vortex shedding frequency follows the Strouhal relation, eq. (7), not being synchronized with the natural frequency of the structure. Since, for this range, the fluid velocity is fairly low (below 0.1m/s), the forcing frequency is also very low and the periods are high, although the amplitudes of motions and forces are very low. As an example, in V=0.08m/s, for which $V_{r0} \cong 3.0$,. the vortex shedding frequency is 0.015Hz corresponding to a period of approximately 86s.

The next plot, Figure 6, presents a time series of cross-flow motions when the reduced velocity is $V_{r0} \cong 3.0$ (flow velocity is 0.08m/s) compared with a time series of cross-flow motions when the reduced velocity is $V_{r0} \cong 14.0$ (flow velocity is 0.26m/s).

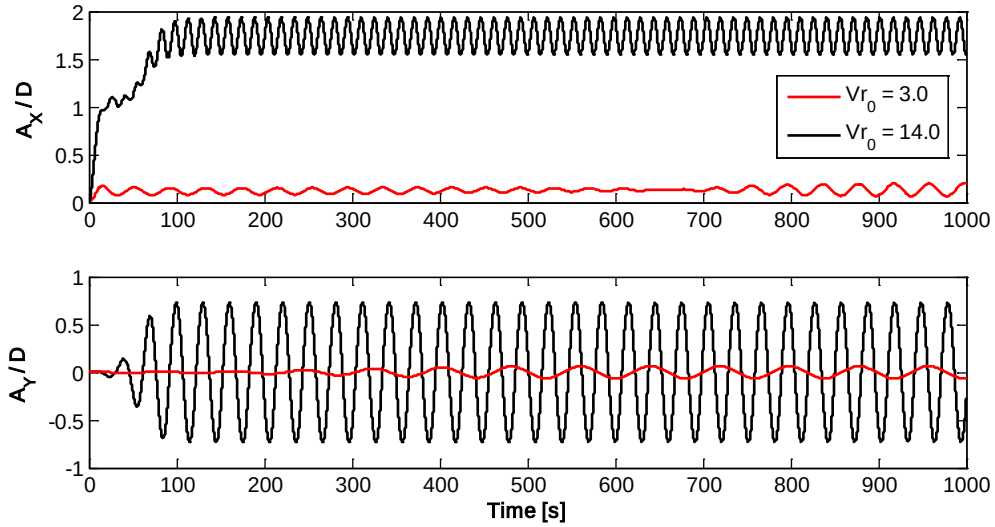

Figure 6: Time series of reduced cross-flow displacement at flow velocity V=0.08m/s and L/D=0.4

It is clear that the period coincides with the period obtained from the Strouhal relation, approximately 86s.

3.2. Variation of structural damping

The next plots present the results obtained by varying the structural damping. This parameter is not easy to be measured because it should be necessary to perform a decay test in air with the structure supported by the springs; however, it is known that the damping is very small.

The following plots, Figure 7 and Figure 8, are the cross-flow and inline motions.

It is clear that the structural damping up to around 8% is not very representative as motions do not increase very much. As of 40%, it seems to be more representative as the increase of motions is larger.

The next plot, Figure 9, presents the results of added mass for different structural damping values.

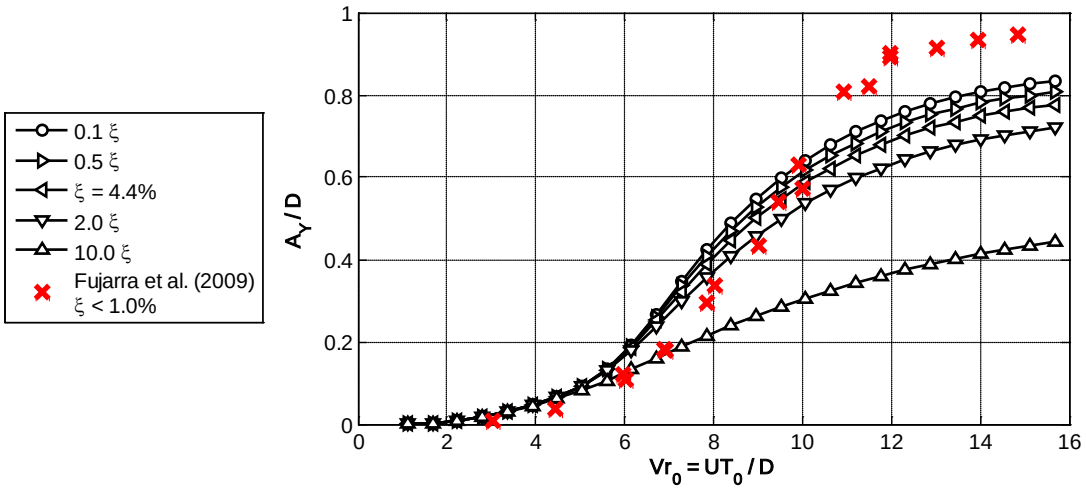

Figure 7: Cross-flow response for different structural damping values. Red points are results from model tests

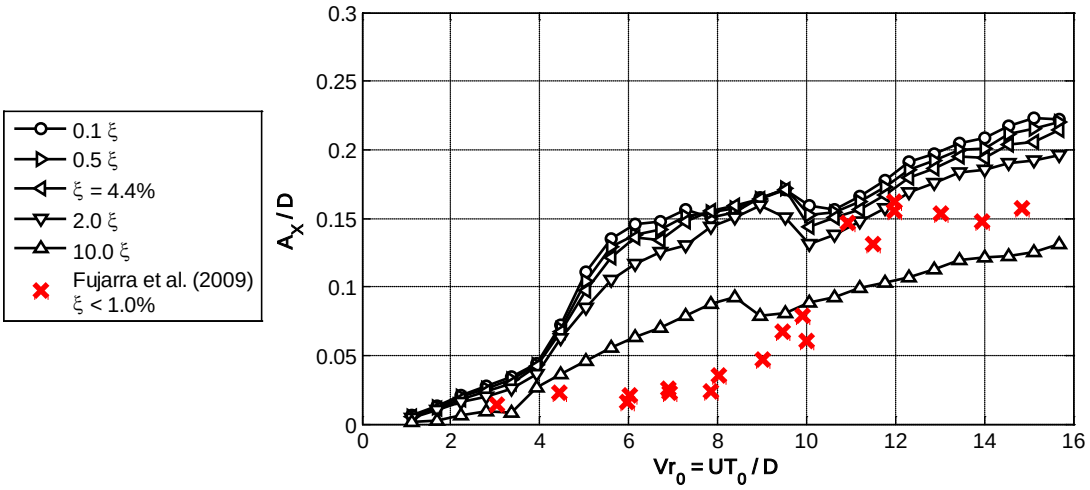

Figure 8: Inline response for different structural damping values. Red points are results from model tests

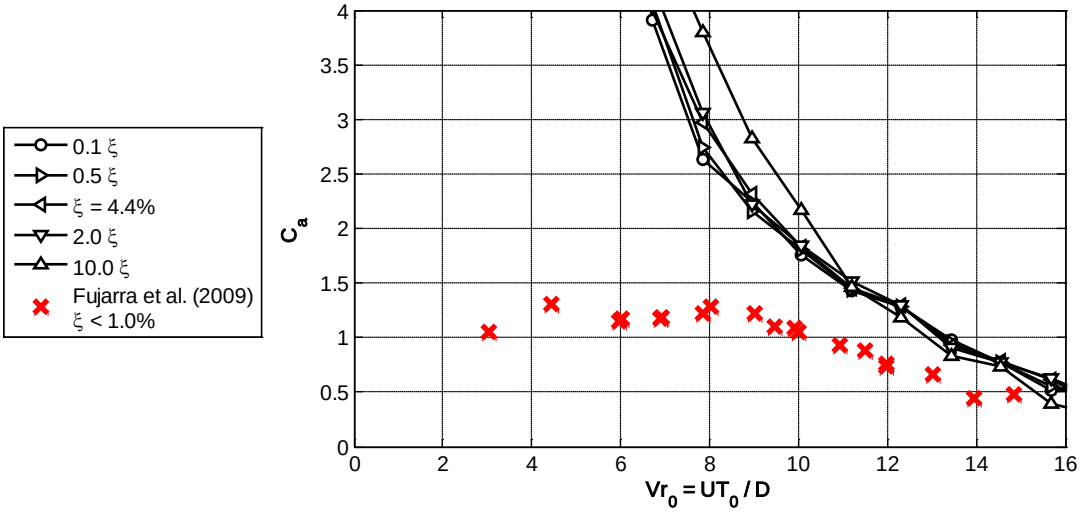

Figure 9: Added mass for different structural damping values. Red points are results from model tests

Very little change is observed when structural damping is varied.
Figure 10 and Figure 11 present the period of oscillations in cross-flow and inline directions, respectively.

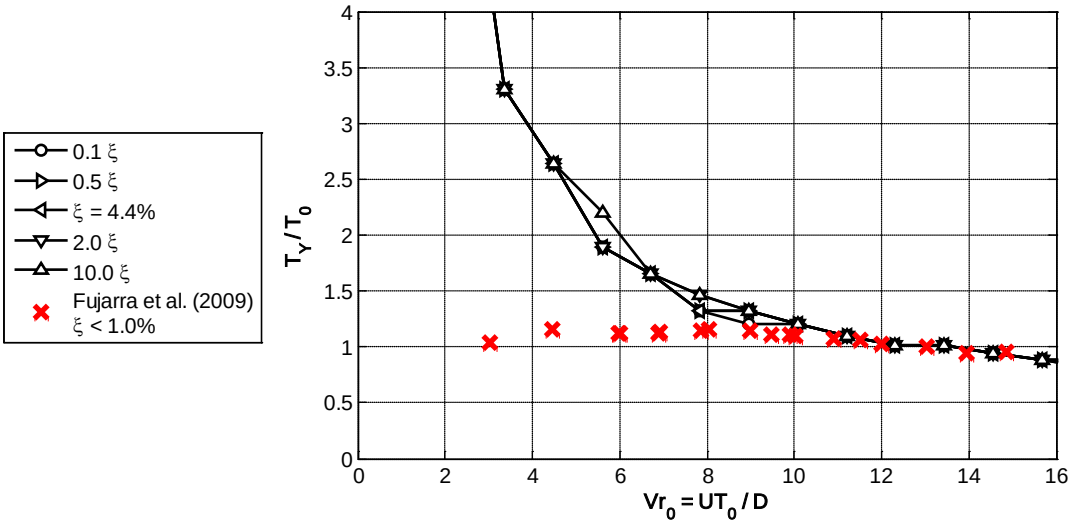

Figure 10: Cross-flow period of oscillation over natural period for different structural damping values. Red points are results from model tests

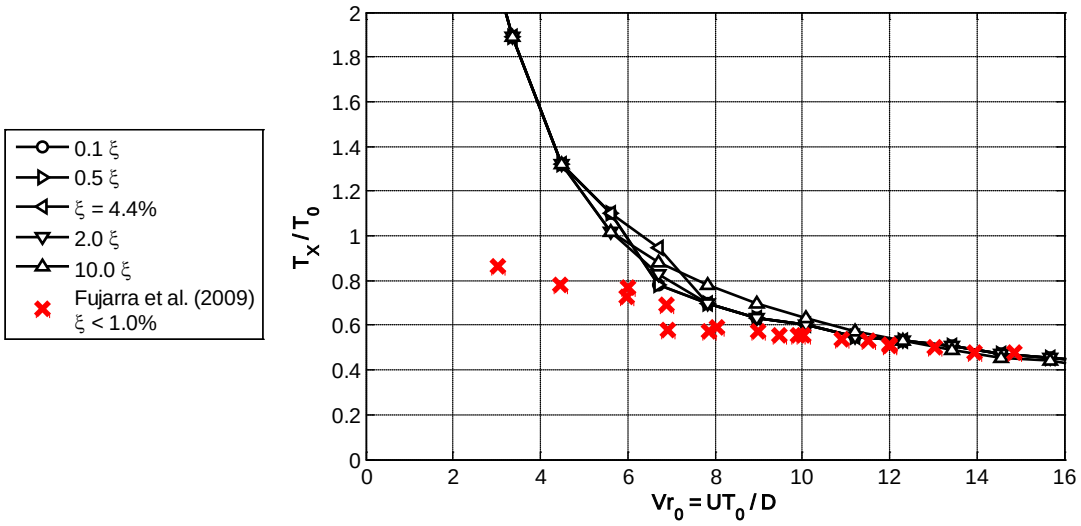

Figure 11: Inline period of oscillation over natural period for different structural damping values. Red points are results from model tests

Once again, very little change is observed when the structural damping is varied as far as periods are concerned.

3.4. Variation of fluid damping

The fluid damping models effects of viscous damping caused by the motion of the structure, relative to the fluid while oscillating. It is difficult to obtain this parameter from the model test as it is not possible to separate the damping effects caused by vortex-shedding from those caused by the motion of the body relative to the fluid. One alternative to do so, and obtain a fluid damping coefficient, is to perform a decay test with fluid velocity.

It is very clear that fluid damping should be a function of motion amplitude. However, it is here taken as constant for the sake of simplicity.

The next plots, Figure 12 and Figure 13, present the cross-flow and inline motions when fluid damping is varied.

The variation of damping causes large variation of response and, as expected, an increase of damping causes a decrease in the motions.

The following plot, Figure 14, presents added mass for varying fluid damping.

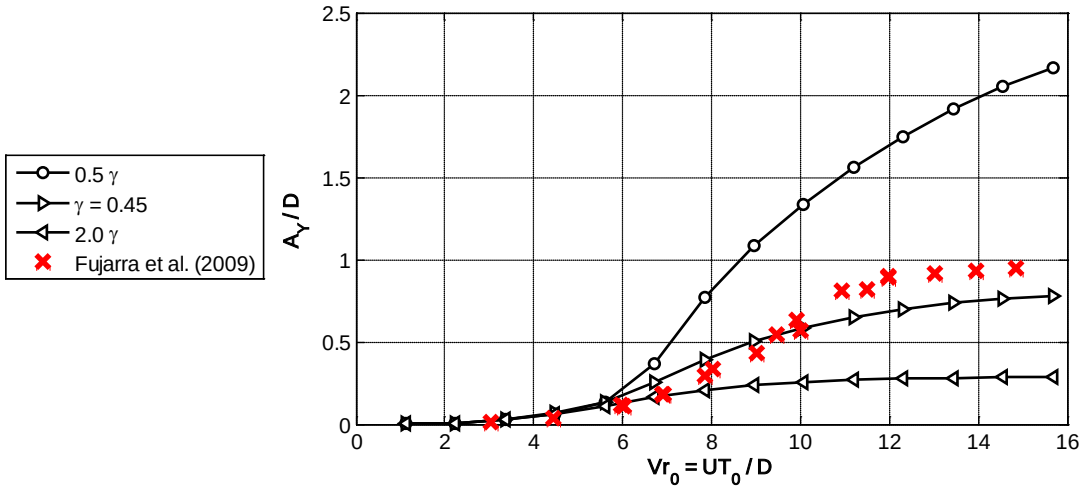

Figure 12: Cross-flow response for fluid damping values. Red points are results from model tests

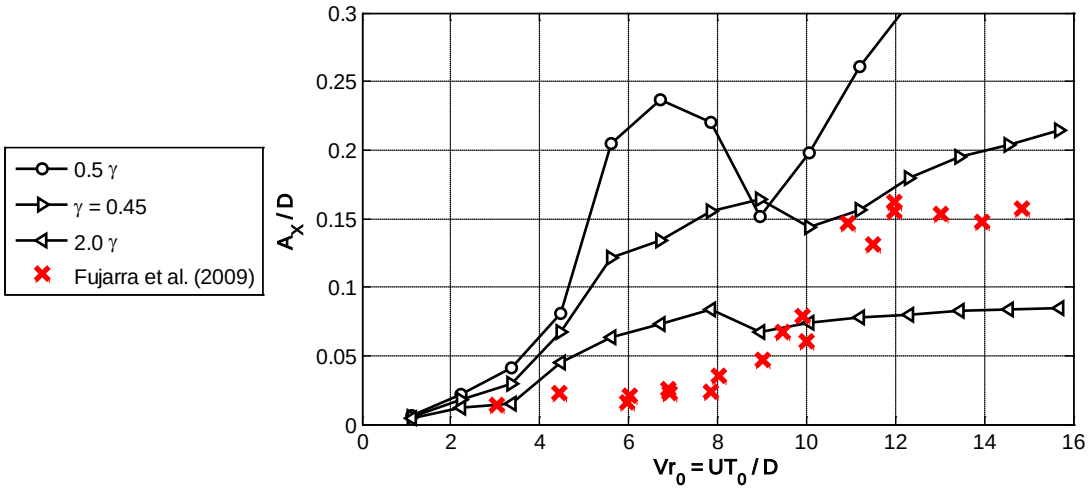

Figure 13: Inline response for different fluid damping values. Red points are results from model tests

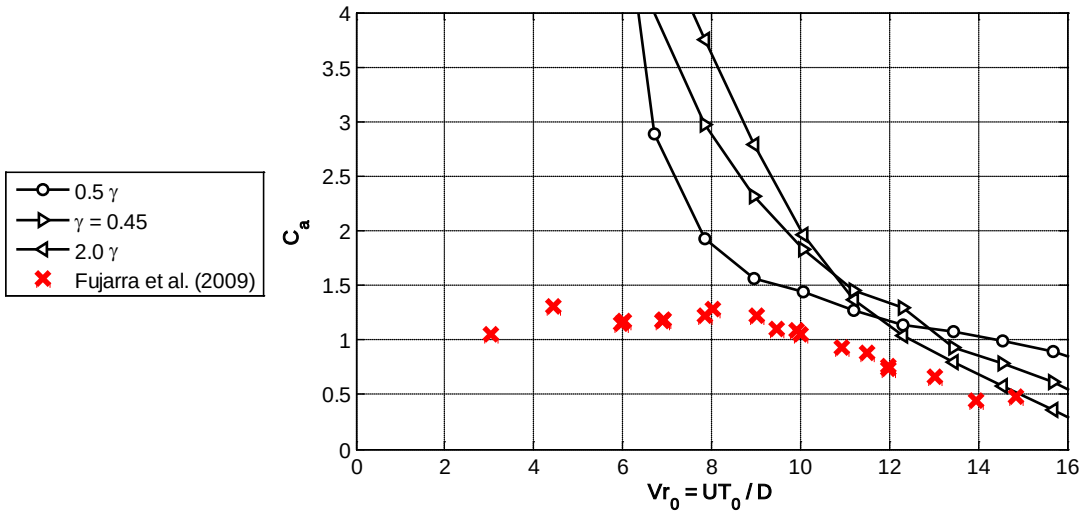

Figure 14: Added mass for different fluid damping values. Red points are results from model tests

A large variation in added mass is also obtained when varying the fluid damping, as presented in Figure 15. Figure 15 and Figure 16 present the variation of the period of oscillations.

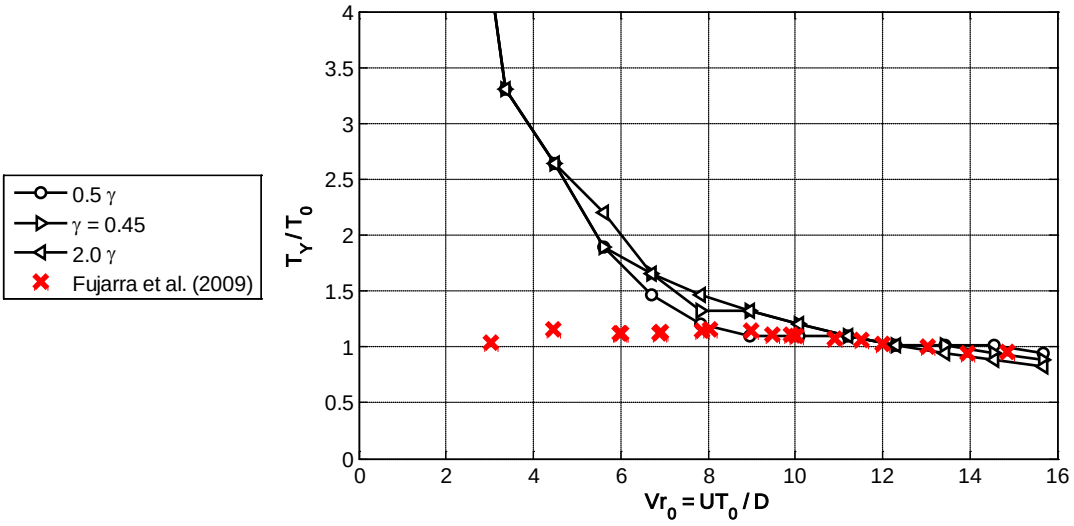

Figure 15: Cross-flow period of oscillation over natural period for different fluid damping values. Red points are results from model tests

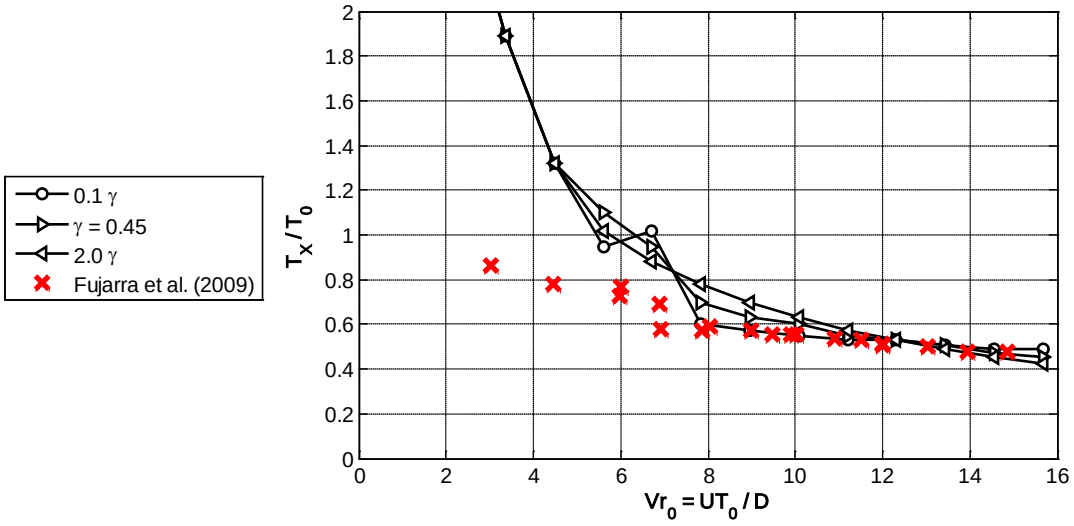

Figure 16: Inline period of oscillation over natural period for different fluid damping values. Red points are results from model tests

It can be noticed that the periods are less impacted by the change in damping in comparison with the previous results. This fact is consistent with the model development since the damping has no direct correlation with the motion frequencies calculation. It is clear that the double frequency relation between inline and cross-flow remained preserved in this case.

3.5. Variation of Strouhal number

The Strouhal number is defined as a dimensionless constant proportional to the predominant vortex shedding frequency and flow velocity, multiplied by the characteristic diameter of the cylinder. It is common to assume that the Strouhal number is a function of the Reynolds number. However, in accordance with some researchers, such as Fox, T.A. and West, G.S. (1993), it is possible to argument that, for cylinders with low aspect ratio (below 13), the Strouhal number is also influenced by this parameter, as presented in Fujarra, A.L.C. *et al.* (2009), in which the obtained Strouhal number is as low as 0.078.

So far, it is premature to state that this actually occurs, however, one could expect that the shedding frequency is not constant along the span and that 3-D effects strongly influence the vortex-shedding patterns and, therefore, the Strouhal number.

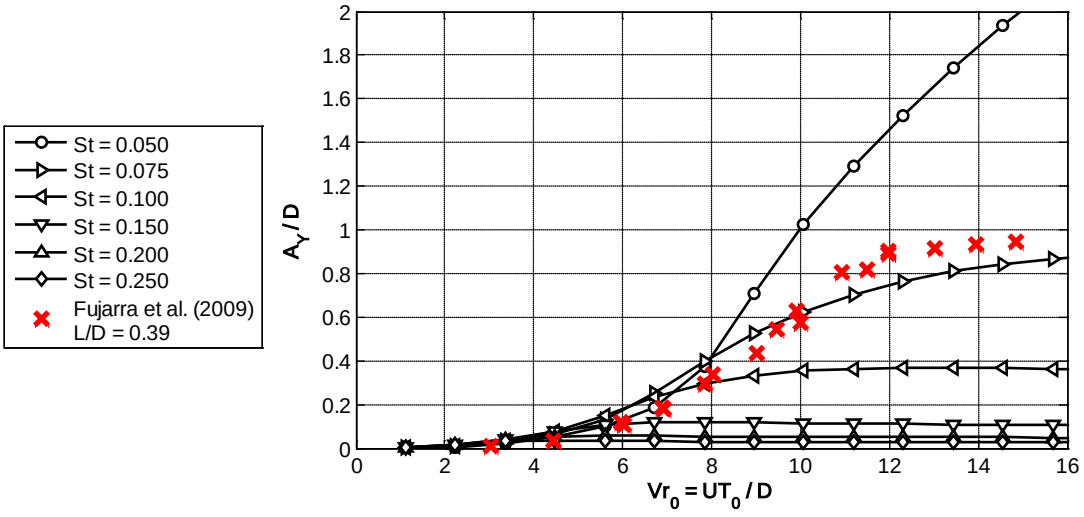

Figure 17: Cross-flow response for different Strouhal numbers values. Red points are results from model tests

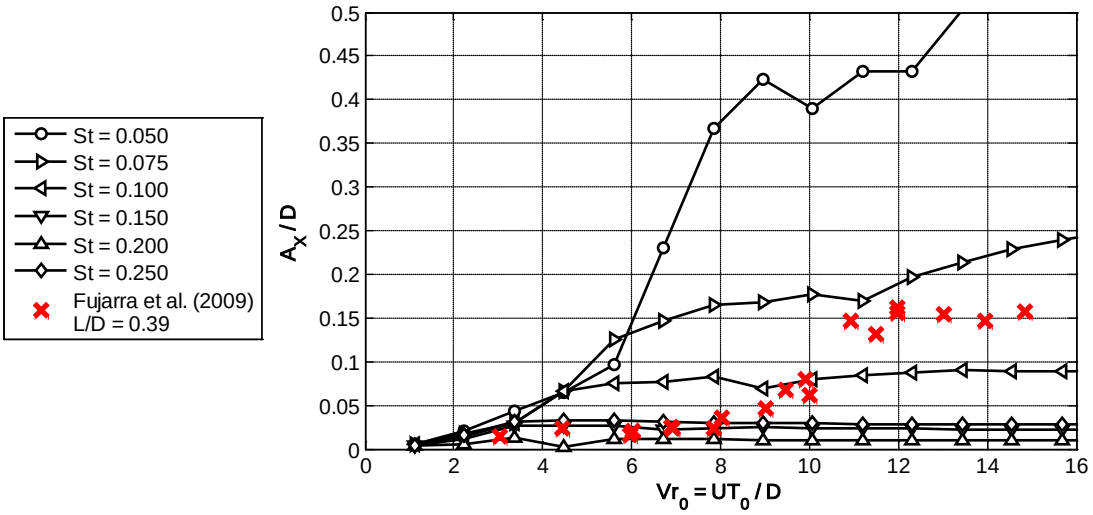

Figure 18: Inline response for different Strouhal numbers. Red points are results from model tests

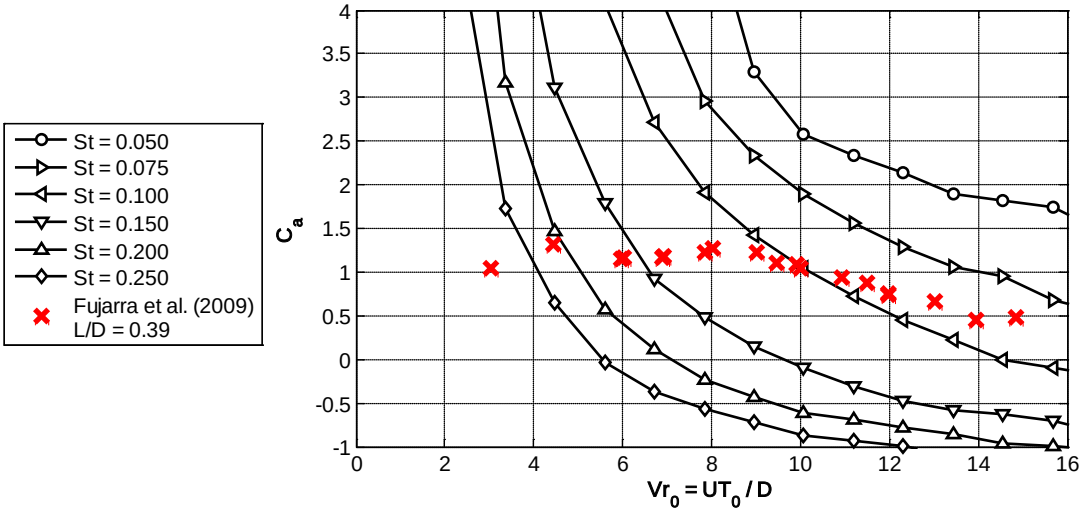

Figure 19: Added mass for different Strouhal numbers. Red points are results from model tests

It is also possible to argument that the vortex shedding pattern is not constant even looking at one aspect ratio in a small range of reduced velocities.

The next plots, Figure 17 and Figure 18, present cross-flow and inline motions when varying the Strouhal number.

It is clear that this parameter is essential for modeling the phenomenon since substantial variation in motions is observed. Since the parameter is related to vortex shedding pattern, and periodicity, a thorough experimental investigation needs to be performed, aiming to obtain vortex shedding frequencies and patterns for small aspect ratios. This investigation is being currently performed.

Figure 19 presents the added mass obtained from varying the Strouhal number.

There is a large variation on the added mass caused by variation of Strouhal number. It is important to notice that, once the Strouhal approaches 0.2, the added mass approaches the value -1, common result for infinite cylinders. On the other hand, when the aspect ratio is below 0.1, the added mass approaches 0. This is also a subject that requires further experimental investigation, i.e., added mass of low aspect ratio cylinders.

In Figure 20 and Figure 21 are presented the periods of oscillation when the Strouhal number varies.

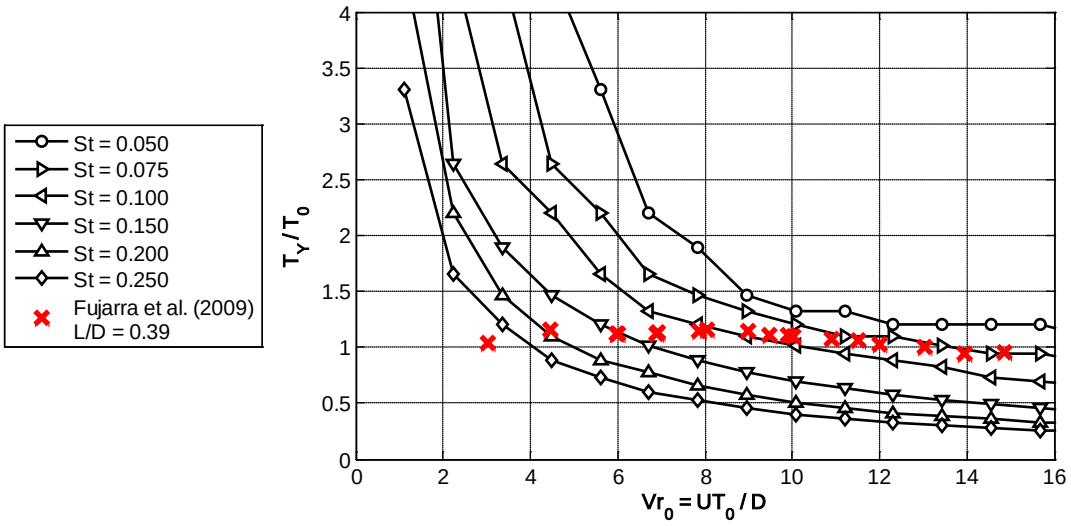

Figure 20: Cross-flow period of oscillation over natural period for different Strouhal numbers. Red points are results from model tests

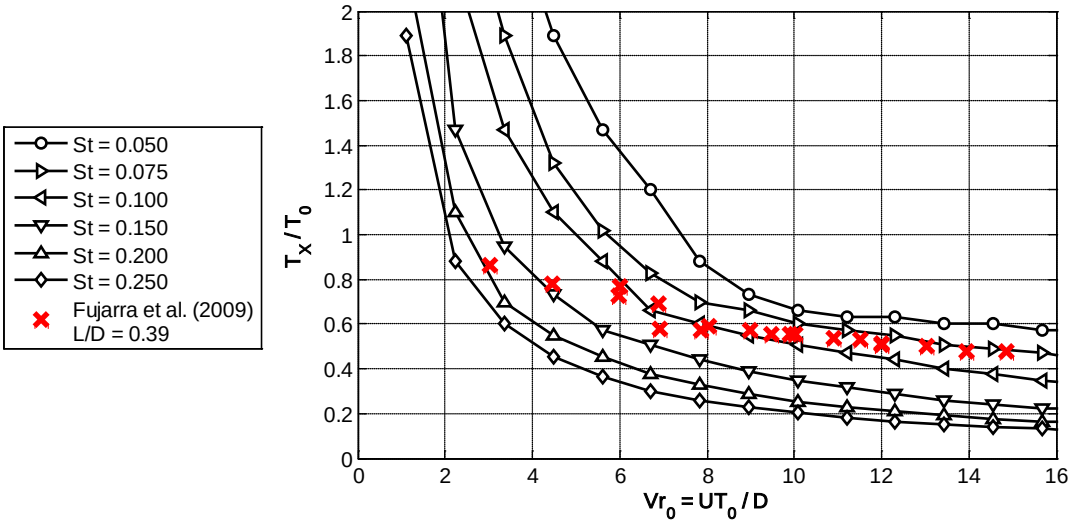

Figure 21: Inline period of oscillation over natural period for different Strouhal numbers. Red points are results from model tests

This was the only parameter capable to influence substantially the period of oscillations, suggesting that it is strongly related to the physics of the phenomenon. Experimental data relating the Strouhal number to the aspect ratio will be very useful in order to model the phenomenon correctly.

4. CONCLUSIONS

A systematic investigation within a range of meaningful parameters was performed and the results compared and discussed. The aim was to draw some conclusions about the modeling itself, identifying merits and deficiencies in order to improve it, but also to draw some conclusions about some characteristics of the phenomenon, identifying the aspects which are not profoundly comprehended and pointing out the direction for further experimental investigations.

Firstly, the aspect ratio was investigated. This subject was raised by the research team during experiments with a monocolumn platform which presents low aspect ratio (L/D < 1). There is a strong belief that the aspect ratio has great influence on the phenomenon mainly due to 3-D effects caused by the vortices shed at the bottom of the structure and the interaction with the vortices shed along the span. Experimental and numerical results show that larger aspect ratios cause an increase in the motions. Added mass is also strongly influenced by the aspect ratio as the asymptotic limit is no longer -1 as in common VIV (great aspect ratio cylinders) but 0, instead . Coherently, the added mass for shorter structures drops more slowly than for the longer ones, inducing smaller motions. The periods of oscillations, however, display similar behavior in all cases.

After that, an investigation was performed on the structural and fluid damping components. This approach was important to highlight some aspects of the modeling and experiment, such as the small influence of the structural damping on the motions of the structure and, on the other hand, the large effect of the fluid damping on them. As commented before, the fluid damping is a function of the amplitude of motion, but **it** was here taken as constant. Perhaps, better results would be achieved if such modeling was performed.

The last parameter investigated was the Strouhal number. This parameter is related to the characteristics of the vortex shedding. Considering short aspect ratio cylinders, the parameter showed to be essential to the comprehension of the phenomenon and in this particular situation the usual 0.2 value may be incorrect. The group has concluded that the parameter should be a function of the aspect ratio due to the 3-D effects and, perhaps also it may not be constant within the range of synchronization because of the tri-dimensionality and interaction between the body and the wake. During the experiments with the monocolumn platform presented in Fujarra, A.L.C. *et al.* (2009), a 0.078 Strouhal number was reported, but this was indirectly calculated during the peak response, where the shedding frequency is considered equal to the oscillating frequency. It is important to obtain the actual shedding frequency over a larger domain through direct measuring. This is being currently perfomed.

Due to its simplicity and easy to use, the van der Pol´s equations showed to be practical to model VIM and to give some insight about the phenomenon, identifing important aspects to look at during experiments. According to that, fundamental experiments are being performed aiming to obtain more information on the subject and shall be important to answer some of the questions raised.

5. ACKNOWLEDGEMENTS

The authors are indebted to the Department of Naval Architecture and Ocean Engineering of the University of São Paulo, mainly to the TPN (Numerical Towing Tank) Laboratory.

6. REFERENCES

Blevins, R. (1990). *Flow-Induced Vibrations*. Malabar, Florida: Krieger Plublishing Company.

Facchinetti, M., Langre, E. d., & Biolley, F. (2004). *Coupling of Structure and Wake Oscillators in Vortex-Induced Vibrations*. Journal of Fluids and Structures , pp. 123-149.

Fox, T. A., & West, G. S. (1993). *Fluid-Induced Loading of Cantilevered Circular Cylinders in a Low-Tubulence Uniform Flow. Part 1: Mean Loading with Aspect Ratios in the Range 4 to 30*. Journal of Fluids and Structures , pp. 1-14.

Fujarra, A. L., & Pesce, P. C. (2002). *Added mass of an Elastically Mounted Rigid Cylinder in Water Subjected to Vortex-Induced Vibrations*. Proceedings of 21st International Offshore Mechanics and Artic Engineering Conference. OMAE2002-28375 .

Fujarra, A. L., Gonçalves, R. T., Faria, F., Nishimoto, K., Cueva, M., & Siqueira, E. F. (2009). *Mitigation of Vortex-Induced Motions of a Monocolumn Platform.* Proceedings of the 28th International Conference on Offshore Mechanics and Arctic Engineering. OMAE2009-79380 .

Furnes, G. (2000). *On Marine Riser Response in Time-and Depth-Dependent Flows*. Journal of Fluids and Structures , pp. 257-273.

Furnes, G., & Sorensen, K. (2007). *Flow Induced Vibrations by Coupled Non-Linear Oscillators*. International Offshore and Polar Engineering Conference , pp. 2781-2787.

Gonçalves, R. T., Fujarra, A. L., Rosetti, G. F., Nishimoto, K., Cueva, M., & Siqueira, E. F. (2009). *Vortex-Induced Motion of a Monocolumn Platform: New Analysis and Comparative Study*. Proceedings of the 28th International Conference on Offshore Mechanics and Artic Engineering. OMAE2009-79378

Gonçalves, R. T., Rosetti, G. F., Fujarra, A. L., Nishimoto, K., & Ferreira, M.D. (2009). *Relevant Aspects in Vortex-Induced Motions of Spar and Monocolumn Platforms: A Brief Overview*. Proceedings of the 20th International Congress of Mechanical Engineering. COB09-0581

Rosetti, G.F., Gonçalves, R.T., Fujarra, A.L.C., Nishimoto, K. & Ferreira, M.D. (2009). *A Phenomenological Model for Vortex-Induced Motions of the Monocolumn Platform and Comparison with Experiments*. Proceedings of the 28th International Conference on Ocean, Offshore and Arctic Engineering. OMAE2009-79431.

Vikestad, K., Vandiver, J. K., & Larsen, C. M. (2000). *Added Mass and Oscillation Frequency for a Circular Cylinder Subjected to Vortex-Induced Vibrations and External Disturbance*. Journal of Fluids and Structures , pp. 1071-1088.

7. RESPONSIBILITY NOTICE

The authors are the only responsible for the printed material included in this paper.